

Article

Matrix-Matched Iron-Oxide Laser Ablation ICP-MS U-Pb Geochronology Using Mixed Solution Standards

Liam Courtney-Davies ^{1,*}, Zhiyong Zhu ^{1,2}, Cristiana L. Ciobanu ¹, Benjamin P. Wade ³, Nigel J. Cook ¹, Kathy Ehrig ⁴, Alexandre R. Cabral ⁵ and Allen Kennedy ⁶

¹ School of Chemical Engineering, The University of Adelaide, Adelaide, SA 5005, Australia; zhiyong.zhu@adelaide.edu.au (Z.Z); cristiana.ciobanu@adelaide.edu.au (C.L.C.); nigel.cook@adelaide.edu.au (N.J.C.)

² State Key Laboratory for Mineral Deposits Research, Department of Earth Sciences, Nanjing University, Nanjing 210093, China

³ Adelaide Microscopy, The University of Adelaide, Adelaide, SA 5005, Australia; Benjamin.wade@adelaide.edu.au

⁴ BHP Billiton Olympic Dam, Adelaide, SA 5000, Australia; Kathy.J.Ehrig@bhpbilliton.com

⁵ Lagerstätten und Rohstoffe, Technische Universität Clausthal, Adolph-Roemer-Str. 2A, Clausthal-Zellerfeld D-38678, Germany; alexandre.cabral@tu-clausthal.de

⁶ John de Laeter Centre, Curtin University of Technology, Bentley, WA 6102, Australia; A.Kennedy@exchange.curtin.edu.au

* Correspondence: liam.courtney-davies@adelaide.edu.au; Tel.: +61-8-8313-4645

Academic Editor: Antonio Simonetti

Received: 18 May 2016; Accepted: 16 August 2016; Published: 23 August 2016

Abstract: U-Pb dating of the common iron-oxide hematite ($\alpha\text{-Fe}_2\text{O}_3$), using laser-ablation inductively-coupled-plasma mass-spectrometry (LA-ICP-MS), provides unparalleled insight into the timing and processes of mineral deposit formation. Until now, the full potential of this method has been negatively impacted by the lack of suitable matrix-matched standards. To achieve matrix-matching, we report an approach in which a U-Pb solution and ablated material from 99.99% synthetic hematite are simultaneously mixed in a nebulizer chamber and introduced to the ICP-MS. The standard solution contains fixed U- and Pb-isotope ratios, calibrated independently, and aspiration of the isotopically homogeneous solution negates the need for a matrix-matched, isotopically homogenous natural iron-oxide standard. An additional advantage of using the solution is that the individual U-Pb concentrations and isotope ratios can be adjusted to approximate that in the unknown, making the method efficient for dating hematite containing low (~10 ppm) to high (>1 wt %) U concentrations. The above-mentioned advantage to this solution method results in reliable datasets, with arguably-better accuracy in measuring U-Pb ratios than using GJ-1 Zircon as the primary standard, which cannot be employed for such low U concentrations. Statistical overlaps between $^{207}\text{Pb}/^{206}\text{Pb}$ weighted average ages (using GJ-1 Zircon) and U-Pb upper intercept ages (using the U-Pb mixed solution method) of two samples from iron-oxide copper-gold (IOCG) deposits in South Australia demonstrate that, although fractionation associated with a non-matrix matched standard does occur when using GJ-1 Zircon as the primary standard, it does not impact the $^{207}\text{Pb}/^{206}\text{Pb}$ or upper intercept age. Thus, GJ-1 Zircon can be considered reliable for dating hematite using LA-ICP-MS. Downhole fractionation of $^{206}\text{Pb}/^{238}\text{U}$ is observed to occur in spot analyses of hematite. The use of rasters in future studies will hopefully minimize this problem, allowing for matrix-matched data. Using the mixed-solution method in this study, we have validated a published hematite Pb-Pb age for Olympic Dam, and provide a new age (1604 ± 11 Ma) for a second deposit in the same province. These ages are further evidence that the IOCG mineralizing event is tied to large igneous province (LIP) magmatism in the region at ~1.6 Ga.

Keywords: iron-oxide; U-Pb geochronology; matrix-matched standard; LA-ICP-MS

1. Introduction

Laser-ablation inductively-coupled plasma mass-spectrometry (LA-ICP-MS) allows the user to rapidly obtain accurate geochronological data [1,2]. The caveat to this is the requirement of certified matrix-matched reference materials, which do not exist for a large number of potentially dateable minerals (unless it can be demonstrated that the effects of using a non-matrix-matched standard are smaller than the propagated errors). This includes the common iron-oxide, hematite (α -Fe₂O₃), which, until now, has only been dated by the U-Pb method using the reference material GJ-1 Zircon [1] as the primary external standard [3]. Analysis of uranium-bearing (up to several wt % U) hematite from Olympic Dam (OD), South Australia, returned dates for hematite mineralization in two samples (1577 ± 5 and 1590 ± 8 Ma) [3]. These are in good agreement with U/Pb zircon ages from OD [4,5]. Ciobanu et al. (2013) [3], thus, argued that the utilization of the GJ-1 Zircon standard is sufficiently reliable for exploratory Fe-oxide geochronological applications.

The analytical approach used by Ciobanu et al. (2013) [3] did not employ a matrix-matched standard, and, thus, only $^{207}\text{Pb}/^{206}\text{Pb}$ dates could be considered reliable due to the relatively low matrix-dependent fractionation effects on Pb-Pb ratios. Accurate U/Pb ages could not be well constrained, as the matrix effects on the measured U/Pb ratios in hematite were largely unknown when standardizing to a non-matrix-matched standard, such as zircon. These matrix effects include phenomena such as laser-induced elemental fractionation, resultant plasma loading and ionization [5–7]. The present study aims at circumventing this problem by using an alternative, mixed solution-solid type of standard for U/Pb dating using LA-ICP-MS. This concept has been tested successfully for U/Pb dating of zircon and baddeleyite [8–10], and non-matrix-matched trace element determination [11,12], and is here applied to dating of U-bearing hematite for the first time. The aims of this study were to: Evaluate the potential of hematite as a U-Pb geochronometer; to assess the effect of “matrix effects” when using a non-matrix matched standard, such as zircon, by comparison with the data of Ciobanu et al. (2013) [3]; to test whether the method gives reliable ages for hematite with low U concentrations; and to provide an “easy-and-ready to use” method for U/Pb dating of hematite.

2. Experimental Methodology

2.1. Instrumentation

Isotope measurements were determined using a Resonetics 193 ArF M-50 Excimer laser ablation system coupled to an Agilent 7700s ICP-MS, housed at Adelaide Microscopy, University of Adelaide. Analysis parameters included a constant repetition rate of 5 Hz, laser fluence of 4.3–9.4 J/cm², and a beam diameter set between 18 and 60 μm (spot analyses) depending on the size of the analyzed U-bearing zones within the hematite grains and their U concentrations. Spot analyses were chosen due to the small size of the hematite grains, which do not have large enough areas of high U zonation to use line rastering. Data were collected using time-resolved acquisition in fast peak-jumping mode and calculations were carried out using the data reduction software GLITTER [13]. Isotope ratios are presented uncorrected for common lead, with concordia plots generated using Isoplot/Ex 3.75 [14]. Instrument optimization and calibration was performed using NIST-610 standard glass (National Institute of Standards and Technology, U.S. Department of Commerce). Table 1 provides instrument and analysis parameters.

Table 1. Instrument and analysis parameters.

Laser Ablation System		ICP-MS	
Type	ArF Excimer	Type	Agilent 7700
Wavelength	193 nm	Makeup gas	Argon
Repetition Rate	5 Hz	Peltier chamber temperature	2 °C
Spot diameter	18–60 µm	Plasma RF power	1550 W
Solution standard	U-Pb	Acquisition mode	TRA
He gas flow	0.55 L·min ⁻¹	Detector mode	Dual Range
Laser Fluence	4.3–9.4 J/cm ²	Dwell Time	
Solution Nebulization		²⁰⁴ Pb	10 ms
Nebulizer	Quartz 250 µL/min	²⁰⁶ Pb	50 ms
Ar carrier gas flow	0.5 L·min ⁻¹	²⁰⁷ Pb	40 ms
Spray chamber	Custom Cyclonic	²⁰⁸ Pb	30 ms
		²³⁸ U	30 ms

2.2. Experimental Procedure

A typical measurement of the “standard” in this experiment comprises aspiration of a liquid, represented by a U-Pb solution with known isotopic ratios in 2% HNO₃, combined with the ablated aerosol of a pure hematite sample, mounted in a 1-inch diameter epoxy block. Mixing was carried out in a spray chamber, in which the ablated hematite aerosol was fed and mixed with the aspirated and nebulized U-Pb solution. Analysis of unknowns comprised mixing of the ablated unknown aerosol with a pure 2% HNO₃ solution to ensure the same liquid plasma loading between the standard and unknown. Between analysis of standards and unknowns, the solution line was washed with aspirated 5% HNO₃ solution. Figure 1 shows the LA-ICP-MS system setup.

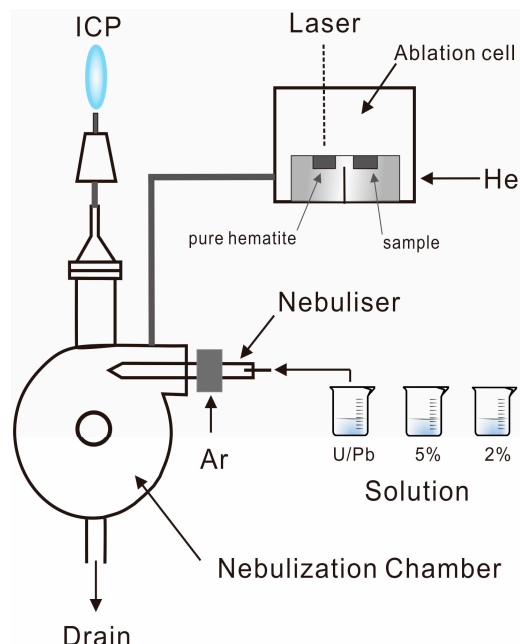


Figure 1. Schematic of the sample introduction system displaying the laser-ablation inductively-coupled plasma-mass spectrometry (LA-ICP-MS) system connected to the U-Pb solution and blank HNO₃ solutions.

2.3. Reagents and Standard Material

The pure hematite analyzed as part of the standard analysis comprised a laboratory-grade synthetic hematite (3–12 mm in size, $\geq 99.98\%$ trace metals basis; Sigma Aldrich Pty. Ltd., St. Louis, MO, USA). The U–Pb calibration solution was made via mixing individual U and Pb single element standard solutions in 2% HNO₃ diluted with Milli-Q water. The Pb isotope ratios of the resultant solution were measured by MC-ICP-MS at Nanjing University, China (Table S1), using added thallium as an internal isotopic standard [15] to correct for mass-dependent isotopic fractionation. Absolute U/Pb concentrations were calibrated via solution ICP-MS on an Agilent 7500cs instrument at Adelaide Microscopy (Table S2). Depending on the U concentration of the sample being analyzed, a stronger or weaker U–Pb solution was made by dilution with 2% HNO₃. The criteria for using different solution strengths were based on the counts-per-second (CPS) registered by the LA-ICP-MS when optimizing the machine parameters.

2.4. Stability and Precision of the Mass Spectrometer

U–Pb mixed standard solutions avoid the potential heterogeneity problems encountered by solid standards. The measured $^{206}\text{Pb}/^{238}\text{U}$ ratio of our solution standard is shown in Figure 2A. To ensure the ^{238}U sensitivity of the unknowns is matched to the standard, pre-ablation of the sample was carried out to assess the ^{238}U CPS. The ^{238}U concentration of the standard was then adjusted appropriately. In our experiment, two concentrations of U–Pb solution (1 and 12 ppb) were employed. The 12-ppb U–Pb mixed solution was used for hematite containing hundreds of ppm U, and the 1-ppb solution was used to calibrate samples that were lower in U (tens of ppm). Each analytical run of 15 unknowns was bracketed by two solution standards.

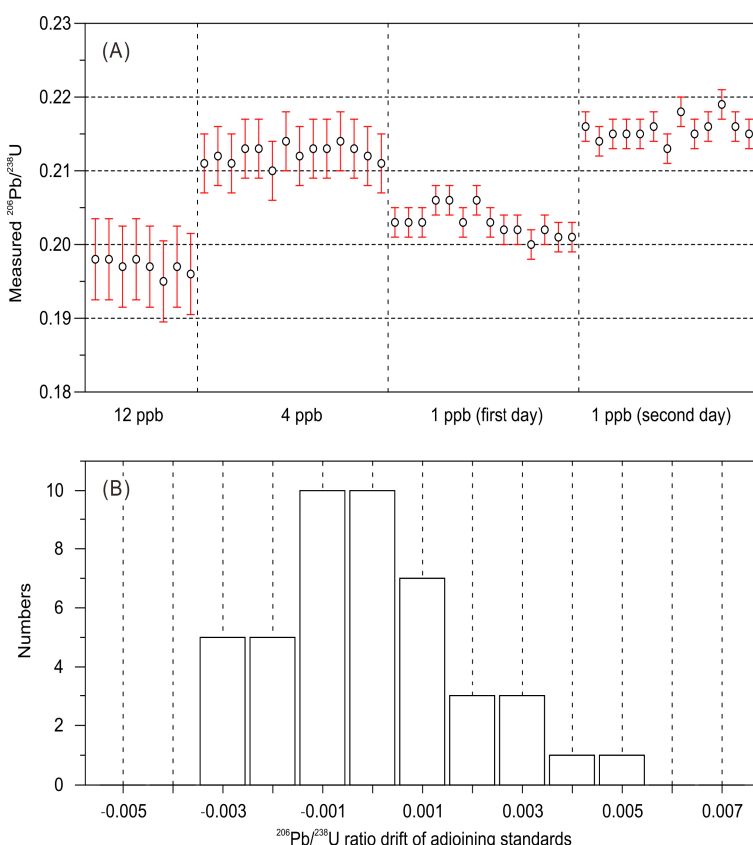


Figure 2. (A) Measured $^{206}\text{Pb}/^{238}\text{U}$ ratios of solution standards with different concentrations; (B) $^{206}\text{Pb}/^{238}\text{U}$ drifts of adjoining standards. The error bars represent 1 sigma standard error.

The total integration time was 60 s, which incorporated 25 s for background collection followed by 35 s for laser firing. This was followed by 40 s for washing. The measured $^{206}\text{Pb}/^{238}\text{U}$ drift over the 23-min period of each run sequence is less than ± 0.003 , which accounts for only 1.5% of the measured ratio (Figure 2B). Although the measured $^{206}\text{Pb}/^{238}\text{U}$ ratio for the same solution can vary day-to-day, the variation within one run is minimal (Figure 2B), allowing the acquisition of high-precision data. In particular, the stability of the 1-ppb mixing solution was still very efficient, even for especially low U samples. Fifteen spots were analyzed on NIST610, immediately following analysis of OD10-4 using just the solution standard calibration method, which gave a 1σ error for the $^{206}\text{Pb}/^{238}\text{U}$ age of 3–4 Ma (<1%), testifying to the stability of the measured signals and instrument at the time of analysis.

2.5. Calibration Process

The $^{207}\text{Pb}/^{206}\text{Pb}$ ratio (0.866312) of the solution standard was measured using MC-ICP-MS with uncertainties of ~0.12%. The $^{206}\text{Pb}/^{238}\text{U}$ ratios (0.286356) were calculated from Q-ICP-MS U/Pb concentration data and MC-ICP-MS Pb isotope ratios; this is expanded upon in Supplementary Text File S1. We assume that the uncertainties of ^{206}Pb and ^{238}U concentrations are 1%; and the propagated 1 sigma deviation of $^{206}\text{Pb}/^{238}\text{U}$ was 1.4%. The uncertainties are then defined in GLITTER (GEMOC Laser ICPMS Total Trace Element Reduction software, Macquarie University, Sydney, Australia) to calibrate the samples. The two ratios from the solution standard were used to calibrate the $^{207}\text{Pb}/^{206}\text{Pb}$ and the $^{206}\text{Pb}/^{238}\text{U}$ ratios of the samples respectively, while the final $^{207}\text{Pb}/^{235}\text{U}$ ratios of the samples were calculated from the calibrated $^{207}\text{Pb}/^{206}\text{Pb}$ and $^{206}\text{Pb}/^{238}\text{U}$.

3. Sample Selection

Hematite samples used in this study are from iron-oxide copper gold (IOCG) deposits in South Australia (Figure 3), and an analogous IOCG province, the Carajás mineral province, Brazil. The Australian samples (i.e., OD10-4 from Olympic Dam and PH-93 from a potentially different tectonic setting within the Olympic Cu-Au Province) contain thousands of ppm to a few wt % U, while the Brazilian sample (CUR-002) has orders of magnitude lower U, but is higher in W (hundreds ppm). Prior to LA-ICP-MS analysis, polished blocks were imaged on an FEI Quanta 450 FEG ESEM, using a back-scattered electron detector optimized to reveal the presence of elevated U and grain-scale zonation in hematite. The samples are all compositionally zoned in uranium (Figure 4), and it is such zones that were targeted for dating.

Sample OD10-4 represents a high-grade ore where the high-U hematite is embedded in bornite (Figure 4A). This is one of ten polished blocks prepared from the same hand specimen, petrographically characterized and analyzed by Ciobanu et al. (2013) [3], who obtained a $^{207}\text{Pb}/^{206}\text{Pb}$ weighted average age of 1577 ± 5 Ma. Sample PH-93 represents hematite breccia cemented with chalcopyrite, and is sourced from an IOCG deposit to the north-nest of Olympic Dam. Although similar in terms of hematite textures to the Olympic Dam material, the high-U zones in PH-93 are coarser (Figure 4B). This sample was also analyzed in this study using GJ-1 Zircon as the primary standard to allow comparison between the two methods. Sample CUR-002 was dated to test the reliability of the mixed solution method with a provincially non-related sample. The sample is from a vein filled with aggregates of coarse lamellar hematite, displaying similar but weaker zoning compared to the two Australian specimens (Figure 4C,D). The vein from which sample CUR-002 was taken crosscuts quartzite and is located some 30 km east north-east of the 1.88 Ga Cigano granite [16], in the ridge that marks the Cinzento strike-slip system of the Carajás mineral province [17].

In addition to providing direct comparison between analysis using GJ-1 Zircon and mixed solution standards, the samples were chosen to assess the age obtained for high-grade ore at OD, to provide a hematite age for associated mineralization elsewhere in the Olympic Cu-Au Province, and to test the application of the method on low-U samples. Ultimately, the choice of samples was designed to illustrate how the method introduced here might find broad application throughout the IOCG province in South Australia and elsewhere.

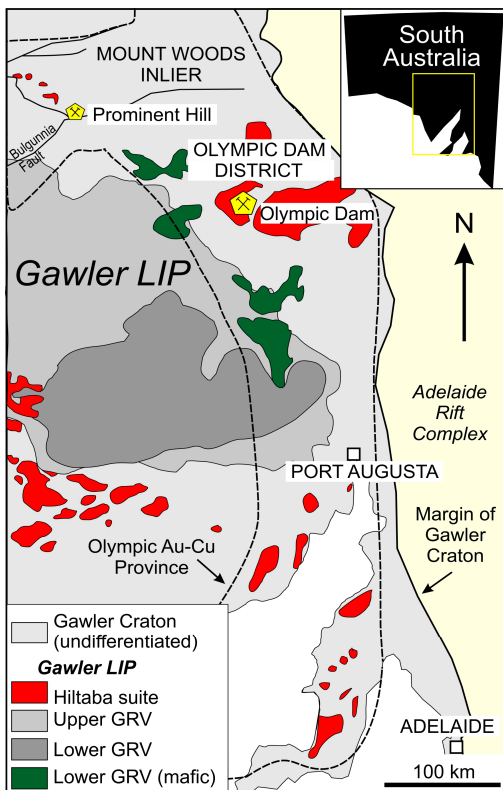


Figure 3. Sketch map showing the location of the Olympic Cu-Au Province within South Australia, as well as exposed Gawler Range Volcanics and Hiltaba Suite intrusive rocks.

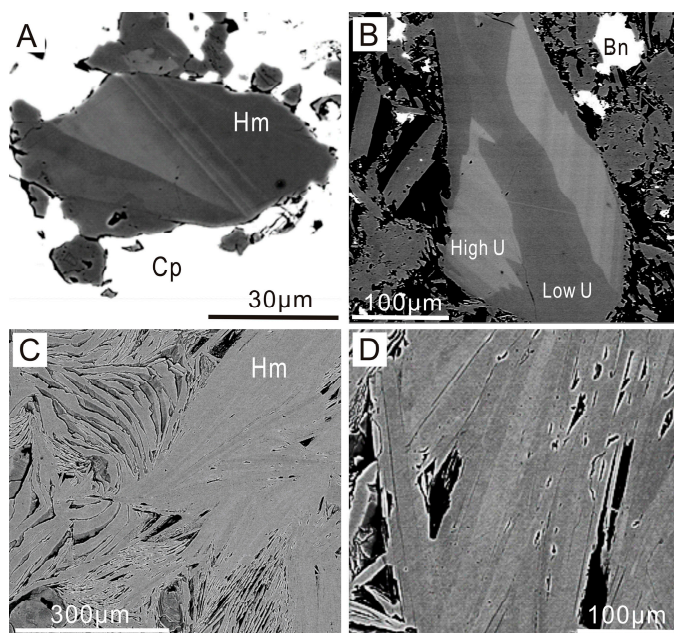


Figure 4. Back scattered electron images of U-bearing zoned hematite. (A,B) Hematite (Hm) displaying oscillatory and sectorial zoning expressed as high-U from Olympic Dam (A) and a second sample from another IOCG deposit in the Olympic Cu-Au Province (B) note differences in size, and coarser zones for the latter. Additionally note association with sulphides, bornite (Bn) and chalcopyrite (Cp), respectively; (C,D) low-U hematite from Carajás (CUR-002) showing aggregates of hematite with zones containing U and W in the centers of the lamellae (brighter on BSE images).

4. U/Pb Geochronology Results

Sample OD10-4 (Table 2, Figure 5) produced a U/Pb upper intercept date of 1595 ± 18 Ma and was anchored to a lower intercept of 0 ± 40 Ma using an $18 \mu\text{m}$ spot size and a 12-ppb mixed solution. None of the spots analyzed in this sample have been excluded from the processed dataset. The data ranges from 100% to 112% concordance, with the discordancy either due to recent Pb loss, or, more likely, due to laser induced elemental fractionation; points plotting above the concordia relate to U loss. Although the error is relatively high, the low amount of points analyzed and inclusion of all points attests to the reliability of the method to generate coherent ages.

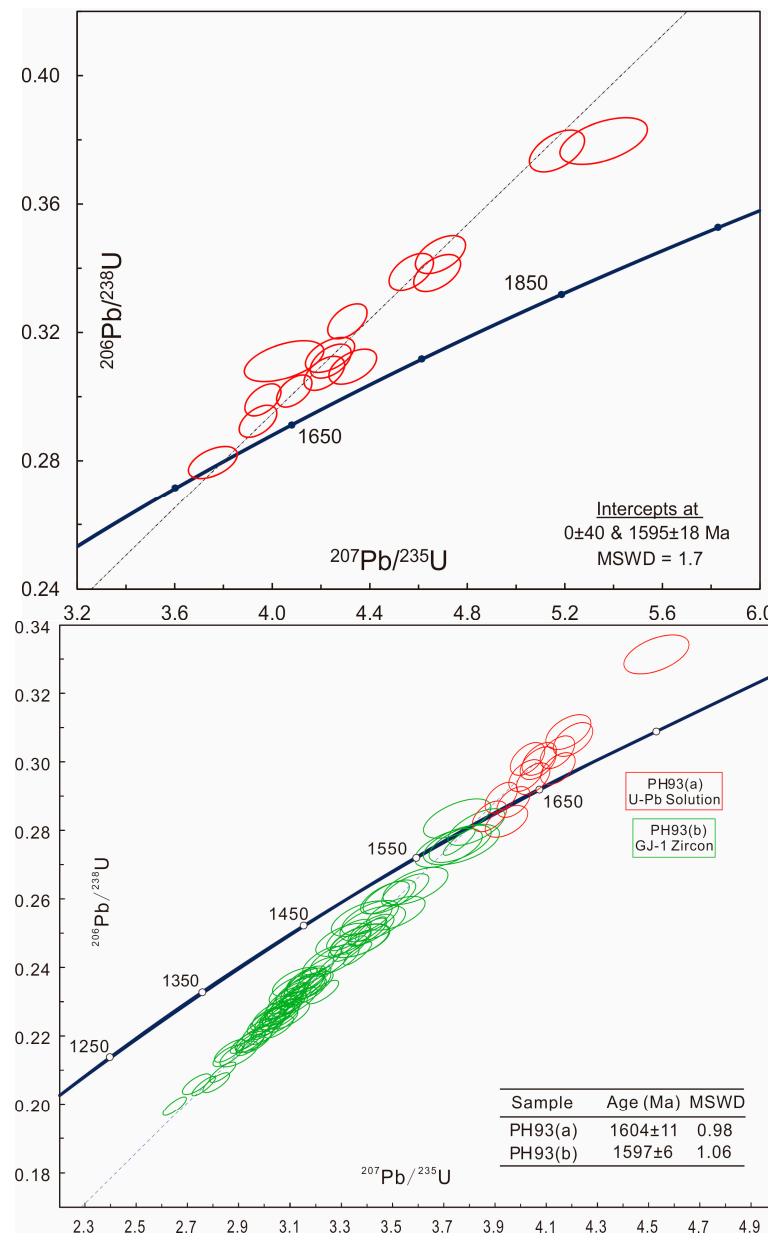


Figure 5. Conventional concordia plots displaying analyzed grains of high-U hematite from the Olympic Province. The first concordia displays sample OD10-4 analyzed through the U–Pb solution method. The second concordia overlays data from sample PH93 collected through the U–Pb solution method (a) and GJ-1 Zircon (b). Data are given in Tables 2–4. Note, all U–Pb solution data plots on or above concordia, whereas all GJ-1 Zircon data plots on or below concordia.

Table 2. Geochronological data for zoned hematite (sample OD10-4) using mixed-solution method.

Spot No.	$^{207}\text{Pb}/^{206}\text{Pb}$	1σ	$^{206}\text{Pb}/^{238}\text{U}$	1σ	$^{207}\text{Pb}/^{235}\text{U}$	1σ	$^{207}\text{Pb}/^{206}\text{Pb}$	1σ	$^{206}\text{Pb}/^{238}\text{U}$	1σ	$^{207}\text{Pb}/^{235}\text{U}$	1σ	Concordancy (%)	^{204}Pb	^{206}Pb	^{207}Pb	^{208}Pb	^{238}U	$^{204}\text{Pb}/^{207}\text{Pb}$	Inc/Exc
1	0.0975	0.0019	0.2795	0.0033	3.7565	0.0662	1577	35	1589	17	1584	16	100	5	33,155	3283	137	171,602	0.0015	Inc
2	0.0978	0.0013	0.2923	0.0033	3.9418	0.0510	1582	24	1653	17	1622	12	102	3	76,344	7580	91	377,715	0.0004	Inc
3	0.0966	0.0012	0.3235	0.0036	4.3083	0.0533	1560	23	1807	18	1695	11	107	0	91,744	8999	52	410,380	0.0000	Inc
4	0.0944	0.0029	0.3111	0.0042	4.0485	0.1076	1516	56	1746	21	1644	24	106	14	12,125	1161	176	56,402	0.0121	Inc
5	0.0961	0.0012	0.2990	0.0033	3.9618	0.0489	1550	23	1686	17	1626	11	104	17	98,322	9589	119	475,862	0.0018	Inc
6	0.1002	0.0014	0.3385	0.0038	4.6762	0.0635	1628	25	1879	19	1763	13	107	0	57,251	5819	169	244,735	0.0000	Inc
7	0.1024	0.0025	0.3796	0.0048	5.3595	0.1186	1668	45	2075	23	1878	21	110	0	10,321	1072	185	39,352	0.0000	Inc
8	0.0988	0.0013	0.3111	0.0035	4.2398	0.0554	1602	24	1746	18	1682	12	104	0	68,567	6873	202	319,022	0.0000	Inc
9	0.0995	0.0013	0.3073	0.0035	4.2137	0.0550	1614	24	1727	18	1677	12	103	5	62,854	6338	539	296,105	0.0008	Inc
10	0.0982	0.0016	0.3130	0.0036	4.2370	0.0666	1590	31	1755	18	1681	14	104	3	31,642	3148	243	146,337	0.0010	Inc
11	0.0983	0.0011	0.3017	0.0033	4.0906	0.0478	1593	21	1700	17	1652	11	103	7	205,525	20,481	174	986,231	0.0003	Inc
12	0.0988	0.0015	0.3442	0.0039	4.6900	0.0679	1602	28	1907	20	1765	14	108	11	44,410	4447	305	186,834	0.0025	Inc
13	0.0996	0.0015	0.3765	0.0043	5.1679	0.0747	1616	28	2060	21	1847	14	112	0	42,844	4321	79	164,804	0.0000	Inc
14	0.1015	0.0016	0.3093	0.0036	4.3303	0.0647	1652	29	1737	18	1699	14	102	0	30,706	3158	229	143,785	0.0000	Inc
15	0.0978	0.0013	0.3389	0.0038	4.5702	0.0602	1583	25	1881	19	1744	12	108	23	51,642	5115	1491	220,769	0.0045	Inc

Table 3. Geochronological data for zoned hematite (sample PH-93) using mixed-solution method.

Spot No.	$^{207}\text{Pb}/^{206}\text{Pb}$	1σ	$^{206}\text{Pb}/^{238}\text{U}$	1σ	$^{207}\text{Pb}/^{235}\text{U}$	1σ	$^{207}\text{Pb}/^{206}\text{Pb}$	1σ	$^{206}\text{Pb}/^{238}\text{U}$	1σ	$^{207}\text{Pb}/^{235}\text{U}$	1σ	Concordancy (%)	^{204}Pb	^{206}Pb	^{207}Pb	^{208}Pb	^{238}U	$^{204}\text{Pb}/^{207}\text{Pb}$	Inc/Exc
1	0.0969	0.0011	0.3013	0.0032	4.0267	0.0444	1566	20	1698	16	1640	10	104	0	115,237	11,217	2	524,174	0.00000	Inc
2	0.1008	0.0011	0.2984	0.0031	4.1449	0.0446	1638	19	1683	16	1663	10	101	0	183,960	18,611	1	845,094	0.00000	Inc
3	0.0991	0.0010	0.3032	0.0032	4.1430	0.0443	1607	19	1707	16	1663	10	103	6	213,122	21,209	8	963,706	0.00028	Inc
4	0.0994	0.0010	0.2954	0.0031	4.0487	0.0431	1613	19	1669	16	1644	10	101	0	265,097	26,461	5	1,230,702	0.00000	Inc
5	0.0980	0.0011	0.3013	0.0032	4.0726	0.0443	1587	20	1698	16	1649	10	103	0	130,179	12,815	0	592,727	0.00000	Inc
6	0.0984	0.0011	0.2964	0.0031	4.0208	0.0443	1594	20	1673	16	1638	10	102	6	141,507	13,980	4	655,082	0.00043	Inc
7	0.0998	0.0011	0.2885	0.0030	3.9717	0.0427	1621	19	1634	16	1628	10	100	0	167,315	16,772	0	795,856	0.00000	Inc
8	0.0982	0.0015	0.3092	0.0034	4.1860	0.0581	1590	27	1737	17	1671	13	104	9	19,282	1900	4	85,593	0.00474	Inc
9	0.0982	0.0010	0.2898	0.0030	3.9241	0.0417	1590	19	1641	16	1619	10	101	0	326,254	32,167	18	1,545,714	0.00000	Inc
10	0.0990	0.0011	0.2843	0.0030	3.8787	0.0443	1605	21	1613	15	1609	10	100	13	134,769	13,391	2	651,199	0.00097	Inc
11	0.0983	0.0011	0.3000	0.0032	4.0680	0.0463	1593	21	1691	16	1648	10	103	6	133,301	13,161	0	610,394	0.00046	Inc
12	0.0993	0.0012	0.3070	0.0033	4.2042	0.0508	1611	23	1726	17	1675	11	103	11	107,235	10,692	21	479,948	0.00103	Inc
13	0.0989	0.0020	0.3322	0.0038	4.5293	0.0839	1604	38	1849	19	1736	17	106	0	20,203	2006	6	83,611	0.00000	Inc
14	0.1012	0.0015	0.2828	0.0031	3.9446	0.0549	1646	27	1605	16	1623	13	99	6	35,223	3578	19	171,296	0.00168	Inc

Table 4. Geochronological data for zoned hematite (sample PH-93) using GJ-1 Zircon as standard, U units are in net integrated counts/s.

Spot No.	$^{207}\text{Pb}/^{206}\text{Pb}$	1 σ	$^{206}\text{Pb}/^{238}\text{U}$	1 σ	$^{207}\text{Pb}/^{235}\text{U}$	1 σ	$^{207}\text{Pb}/^{206}\text{Pb}$	1 σ	$^{206}\text{Pb}/^{238}\text{U}$	1 σ	$^{207}\text{Pb}/^{235}\text{U}$	1 σ	Concordancy (%)	^{204}Pb	^{206}Pb	^{207}Pb	^{208}Pb	^{238}U	$^{204}\text{Pb}/^{207}\text{Pb}$	Inc/Exc	Notes
1	0.0974	0.0016	0.2491	0.0030	3.3457	0.0563	1575.6	31	1434	15	1492	13	91	0	358,124	35,083	0	1,571,490	0.0000	Inc	
2	0.0983	0.0015	0.2288	0.0025	3.1016	0.0457	1592.9	28	1328	13	1433	11	83	34	1,679,299	165,047	57	7,631,865	0.0002	Inc	
3	0.0993	0.0017	0.2507	0.0030	3.4310	0.0585	1611.0	31	1442	15	1512	13	90	47	4,388,089	436,897	1904	19,018,996	0.0001	Inc	
4	0.0991	0.0012	0.2761	0.0025	3.7704	0.0405	1606.6	22	1572	13	1587	9	98	26	641,549	63,493	119	2,066,412	0.0004	Inc	
5	0.0994	0.0015	0.2301	0.0026	3.1542	0.0462	1613.5	27	1335	13	1446	11	83	15	3,612,039	359,811	311	16,437,574	0.0000	Inc	
6	0.0977	0.0016	0.2363	0.0026	3.1819	0.0508	1580.2	31	1367	14	1453	12	87	26	626,242	61,641	34	2,629,886	0.0004	Inc	
7	0.0988	0.0016	0.2268	0.0026	3.0890	0.0491	1601.8	29	1318	14	1430	12	82	12	1,057,774	105,597	246	5,011,429	0.0001	Inc	
8	0.0994	0.0015	0.2347	0.0026	3.2155	0.0464	1612.7	27	1359	13	1461	11	84	13	686,076	68,084	317	2,983,425	0.0002	Inc	
9	0.0983	0.0012	0.2317	0.0021	3.1384	0.0343	1591.3	23	1343	11	1442	8	84	36	481,616	47,324	27	1,806,129	0.0008	Inc	
10	0.0991	0.0013	0.2452	0.0025	3.3499	0.0422	1607.3	25	1414	13	1493	10	88	21	897,793	88,769	126	3,483,487	0.0002	Inc	
11	0.0992	0.0014	0.2500	0.0027	3.4188	0.0485	1609.3	27	1438	14	1509	11	89	43	1,236,666	122,600	265	5,024,110	0.0004	Inc	
12	0.0985	0.0014	0.2311	0.0024	3.1389	0.0411	1596.7	25	1340	12	1442	10	84	11	1,373,742	134,877	23	5,764,943	0.0001	Inc	
13	0.0981	0.0016	0.2241	0.0025	3.0302	0.0492	1588.7	31	1303	13	1415	12	82	29	2,621,084	257,454	521	12,092,409	0.0001	Inc	
14	0.0978	0.0017	0.2462	0.0029	3.3195	0.0566	1582.5	32	1419	15	1486	13	90	34	88,275	8696	9	377,705	0.0039	Exc	a
15	0.0993	0.0019	0.2804	0.0035	3.8364	0.0724	1610.5	35	1594	18	1600	15	99	19	397,112	40,162	164	1,571,576	0.0005	Inc	
16	0.0972	0.0018	0.2600	0.0031	3.4847	0.0620	1571.8	34	1490	16	1524	14	95	0	150,286	14,739	45	614,635	0.0000	Inc	
17	0.0991	0.0012	0.2471	0.0023	3.3736	0.0385	1606.3	23	1423	12	1498	9	89	53	1,036,758	102,851	278	3,725,470	0.0005	Inc	
18	0.0983	0.0017	0.2288	0.0026	3.1005	0.0525	1592.3	32	1328	14	1433	13	83	1	2,603,502	256,726	61	11,838,008	0.0000	Inc	
19	0.0991	0.0013	0.2094	0.0019	2.8612	0.0332	1607.3	24	1226	10	1372	9	76	24	990,138	98,206	53	4,177,061	0.0002	Inc	
20	0.0986	0.0019	0.2421	0.0030	3.2912	0.0623	1598.1	36	1398	15	1479	15	87	60	2,274,552	225,982	215	10,140,658	0.0003	Inc	
21	0.0993	0.0014	0.2208	0.0022	3.0221	0.0403	1610.6	26	1286	12	1413	10	80	25	1,242,696	123,093	74	5,310,694	0.0002	Inc	
22	0.0997	0.0013	0.2064	0.0019	2.8359	0.0339	1618.0	24	1210	10	1365	9	75	11	686,332	68,503	27	2,888,126	0.0002	Inc	
23	0.1004	0.0013	0.2224	0.0020	3.0771	0.0370	1630.6	25	1295	11	1427	9	79	16	1,329,609	133,557	307	5,178,292	0.0001	Inc	
24	0.0995	0.0013	0.2182	0.0020	2.9923	0.0361	1614.6	24	1272	11	1406	9	79	14	1,841,114	183,403	135	7,458,065	0.0001	Inc	
25	0.0980	0.0013	0.2217	0.0021	2.9930	0.0365	1585.4	25	1291	11	1406	9	81	15	1,573,534	154,374	80	6,220,637	0.0001	Inc	
26	0.0990	0.0017	0.2254	0.0025	3.0762	0.0500	1605.1	31	1311	13	1427	12	82	9	1,181,199	116,969	18	5,122,869	0.0001	Inc	
27	0.1029	0.0014	0.2496	0.0024	3.5399	0.0445	1676.4	25	1437	12	1536	10	86	13	209,668	21,612	11	745,289	0.0006	Exc	b
28	0.0993	0.0023	0.2475	0.0032	3.3886	0.0761	1610.9	42	1426	17	1502	18	89	19	1,609,400	162,276	10	7,066,943	0.0001	Inc	
29	0.1002	0.0022	0.2555	0.0032	3.5266	0.0743	1626.8	40	1467	17	1533	17	90	47	1,071,385	108,255	60	4,488,290	0.0004	Inc	
30	0.0988	0.0025	0.2525	0.0035	3.4378	0.0833	1601.6	46	1451	18	1513	19	91	14	1,946,683	195,519	68	8,610,834	0.0001	Inc	
31	0.1006	0.0012	0.2438	0.0022	3.3800	0.0359	1634.5	22	1407	11	1500	8	86	32	562,421	56,764	322	2,025,558	0.0006	Inc	
32	0.0989	0.0012	0.2367	0.0022	3.2255	0.0342	1602.5	22	1370	11	1463	8	85	4	960,716	95,346	13	3,570,458	0.0000	Inc	
33	0.0981	0.0012	0.2273	0.0021	3.0728	0.0328	1587.9	22	1320	11	1426	8	83	18	759,636	74,830	179	2,937,270	0.0002	Inc	
34	0.0988	0.0014	0.2231	0.0023	3.0405	0.0422	1602.4	27	1298	12	1418	11	81	10	444,428	44,200	46	1,912,461	0.0002	Inc	
35	0.1158	0.0014	0.2723	0.0026	4.3452	0.0491	1891.7	22	1552	13	1702	9	82	104	87,658	10,202	5406	286,152	0.0102	Exc	c
36	0.1207	0.0015	0.3719	0.0035	6.1896	0.0706	1966.9	22	2038	16	2003	10	104	202	82,870	10,054	8583	199,203	0.0201	Exc	c
37	0.0997	0.0014	0.3164	0.0027	4.3477	0.0536	1618.2	26	1772	13	1703	10	109	39	360,353	36,098	1705	888,545	0.0011	Exc	c
38	0.0976	0.0015	0.2263	0.0025	3.0452	0.0461	1579.1	28	1315	13	1419	12	83	42	2,915,401	287,873	68	13,379,398	0.0001	Inc	
39	0.0973	0.0015	0.2418	0.0027	3.2435	0.0495	1572.9	29	1396	14	1468	12	89	24	1,084,105	106,636	81	4,645,543	0.0002	Inc	
40	0.0970	0.0016	0.2333	0.0027	3.1184	0.0522	1566.7	31	1352	14	1437	13	86	20	1,166,921	115,101	97	5,317,064	0.0002	Inc	
41	0.0977	0.0015	0.2303	0.0026	3.1028	0.0479	1581.0	29	1336	14	1433	12	85	65	3,206,861	317,610	271	14,493,242	0.0002	Inc	
42	0.0985	0.0016	0.2251	0.0026	3.0580	0.0485	1596.1	30	1309	13	1422	12	82	25	3,258,201	325,873	16	15,085,051	0.0001	Inc	
43	0.0979	0.0016	0.2355	0.0027	3.1780	0.0524	1584.1	31	1363	14	1452	13	86	34	2,438,001	242,741	219	10,914,086	0.0001	Inc	
44	0.0984	0.0018	0.2337	0.0027	3.1695	0.0562	1593.6	34	1354	14	1450	14	85	15	993,572	99,903	83	4,366,896	0.0002	Inc	
45	0.0976	0.0019	0.2602	0.0032	3.5019	0.0669	1579.2	36	1491	17	1528	15	94	15	1,812,700	182,136	143	7,664,977	0.0001	Inc	
46	0.1001	0.0013	0.2242	0.0021	3.0947	0.0365	1626.4	24	1304	11	1431	9	80	29	302,131	30,514	202	1,200,461	0.0010	Inc	
47	0.0993	0.0021	0.2756	0.0036	3.7739	0.0789	1611.3	39	1569	18	1587	17	97	34	1,198,725	122,333	61	4,828,669	0.0003	Inc	
48	0.0982	0.0013	0.2188	0.0020	2.9622	0.0352	1589.9	24	1276	11	1398	9	80	23	1,668,670	165,554	22	6,676,239	0.0001	Inc	
49	0.0990	0.0013	0.2173	0.0020	2.9663</																

Table 4. Cont.

Spot No.	$^{207}\text{Pb}/^{206}\text{Pb}$	1σ	$^{206}\text{Pb}/^{238}\text{U}$	1σ	$^{207}\text{Pb}/^{235}\text{U}$	1σ	$^{207}\text{Pb}/^{206}\text{Pb}$	1σ	$^{206}\text{Pb}/^{238}\text{U}$	1σ	$^{207}\text{Pb}/^{235}\text{U}$	1σ	Concordancy (%)	^{204}Pb	^{206}Pb	^{207}Pb	^{208}Pb	^{238}U	$^{204}\text{Pb}/^{207}\text{Pb}$	Inc/Exc	Notes
51	0.0989	0.0013	0.2260	0.0021	3.0802	0.0376	1602.9	25	1313	11	1428	9	82	22	1,366,690	136,630	12	5,394,476	0.0002	Inc	
52	0.0981	0.0013	0.2263	0.0021	3.0593	0.0377	1587.8	25	1315	11	1423	9	83	13	1,403,969	139,309	31	5,542,698	0.0001	Inc	
53	0.0987	0.0013	0.2182	0.0021	2.9691	0.0371	1599.5	25	1272	11	1400	9	80	22	1,619,038	161,606	44	6,603,413	0.0001	Inc	
54	0.0982	0.0016	0.2343	0.0026	3.1730	0.0511	1590.4	31	1357	14	1451	12	85	11	1,610,758	161,574	29	6,854,733	0.0001	Inc	
55	0.0976	0.0014	0.2250	0.0022	3.0270	0.0387	1578.4	26	1308	11	1415	10	83	18	457,802	45,280	177	1,824,297	0.0004	Inc	
56	0.0970	0.0022	0.2539	0.0034	3.3953	0.0773	1567.3	43	1459	17	1503	18	93	36	4,452,099	443,120	34	19,586,568	0.0001	Inc	
57	0.0972	0.0014	0.2060	0.0020	2.7602	0.0360	1571.2	26	1207	11	1345	10	77	14	959,312	94,476	14	4,158,679	0.0001	Inc	
58	0.0976	0.0014	0.2142	0.0021	2.8808	0.0380	1577.8	26	1251	11	1377	10	79	20	1,450,919	143,445	34	6,049,981	0.0001	Inc	
59	0.0986	0.0014	0.2261	0.0022	3.0741	0.0411	1598.2	27	1314	12	1426	10	82	15	571,895	57,181	82	2,260,135	0.0003	Inc	
60	0.0967	0.0018	0.2356	0.0027	3.1402	0.0582	1560.9	35	1364	14	1443	14	87	19	956,335	95,287	35	4,086,355	0.0002	Inc	
61	0.1052	0.0015	0.2473	0.0027	3.5852	0.0494	1718.0	26	1425	14	1546	11	83	16	254,148	26,922	29	1,046,269	0.0006	Exc	b
62	0.1041	0.0012	0.2105	0.0020	3.0188	0.0328	1697.5	22	1232	10	1412	8	73	6	184,596	19,297	61	782,648	0.0003	Exc	d
63	0.0990	0.0016	0.2346	0.0027	3.1989	0.0513	1605.2	30	1358	14	1457	12	85	4	1,925,329	192,516	55	8,914,925	0.0000	Inc	
64	0.0989	0.0017	0.2147	0.0025	2.9234	0.0484	1602.8	31	1254	13	1388	13	78	9	792,921	79,559	35	3,850,466	0.0001	Inc	
65	0.0976	0.0013	0.2318	0.0025	3.1167	0.0421	1579.0	25	1344	13	1437	10	85	3	1,765,155	173,074	216	7,785,311	0.0000	Inc	
66	0.0997	0.0014	0.2364	0.0026	3.2466	0.0451	1618.1	26	1368	13	1468	11	85	101	1,098,693	110,264	287	4,758,180	0.0009	Exc	c
67	0.0980	0.0014	0.2388	0.0025	3.2225	0.0437	1585.5	26	1380	13	1463	11	87	3	933,955	92,136	299	3,898,835	0.0000	Inc	
68	0.1143	0.0015	0.2331	0.0022	3.6724	0.0423	1868.7	23	1351	11	1565	9	72	17	79,178	9127	999	295,491	0.0019	Exc	a
69	0.0985	0.0012	0.2054	0.0019	2.7877	0.0299	1595.0	22	1204	10	1352	8	76	22	1,439,121	142,793	43	6,191,064	0.0002	Inc	
70	0.0973	0.0012	0.2362	0.0023	3.1664	0.0380	1572.5	23	1367	12	1449	9	87	12	1,175,148	115,582	47	4,740,360	0.0001	Inc	
71	0.0980	0.0013	0.2282	0.0023	3.0837	0.0392	1587.2	25	1325	12	1429	10	83	10	1,054,676	104,286	9	4,487,131	0.0001	Inc	
72	0.0986	0.0017	0.2622	0.0031	3.5627	0.0600	1598.5	31	1501	16	1541	13	94	19	642,983	63,740	115	2,647,484	0.0003	Inc	
73	0.0996	0.0014	0.2243	0.0021	3.0788	0.0396	1616.1	26	1305	11	1427	10	81	23	29,009	2923	59	110,735	0.0079	Exc	a
74	0.0993	0.0022	0.1845	0.0022	2.5247	0.0509	1610.1	40	1092	12	1279	15	68	22	4875	488	19	22,920	0.0451	Exc	a
75	0.0988	0.0016	0.2190	0.0025	2.9815	0.0482	1601.3	30	1277	13	1403	12	80	8	1,979,677	196,785	49	9,503,796	0.0000	Inc	
76	0.0973	0.0012	0.1995	0.0018	2.6761	0.0298	1573.2	23	1173	10	1322	8	75	21	399,834	39,344	144	1,748,439	0.0005	Inc	
77	0.0987	0.0014	0.2291	0.0024	3.1165	0.0439	1599.4	27	1330	13	1437	11	83	0	1,078,987	107,212	210	4,628,883	0.0000	Inc	
78	0.1001	0.0017	0.2259	0.0026	3.1157	0.0518	1626.2	31	1313	14	1437	13	81	16	2,587,938	260,008	462	12,235,322	0.0001	Inc	
79	0.0981	0.0012	0.2321	0.0021	3.1378	0.0353	1587.7	23	1346	11	1442	9	85	14	620,074	61,490	192	2,342,069	0.0002	Inc	
80	0.0992	0.0012	0.2509	0.0023	3.4306	0.0390	1608.8	23	1443	12	1511	9	90	22	455,461	45,655	30	1,607,845	0.0005	Inc	
81	0.0990	0.0013	0.2408	0.0022	3.2874	0.0374	1605.6	23	1391	11	1478	9	87	15	834,712	83,678	19	3,004,981	0.0002	Inc	
82	0.0979	0.0012	0.2179	0.0020	2.9404	0.0336	1583.9	23	1271	11	1392	9	80	20	886,685	87,861	31	3,560,567	0.0002	Inc	
83	0.1012	0.0014	0.2326	0.0023	3.2455	0.0406	1646.0	25	1348	12	1468	10	82	0	476,332	48,675	12	1,865,476	0.0000	Inc	
84	0.0981	0.0013	0.2461	0.0023	3.3268	0.0389	1587.5	24	1418	12	1487	9	89	24	303,591	30,129	12	1,090,386	0.0008	Inc	
85	0.0976	0.0014	0.2102	0.0020	2.8297	0.0361	1579.3	26	1230	11	1363	10	78	14	43,652	4317	7	184,217	0.0032	Exc	a
86	0.0971	0.0014	0.2156	0.0022	2.8871	0.0384	1569.6	26	1259	11	1379	10	80	20	856,148	83,793	50	3,731,805	0.0002	Inc	
87	0.0979	0.0021	0.2542	0.0033	3.4275	0.0721	1584.5	39	1460	17	1511	17	92	23	1,736,866	171,672	17	7,714,529	0.0001	Inc	
88	0.0986	0.0020	0.2328	0.0029	3.1632	0.0640	1598.5	38	1349	15	1448	16	84	21	2,302,525	227,831	27	10,881,509	0.0001	Inc	
89	0.0994	0.0022	0.2475	0.0032	3.3875	0.0744	1612.1	41	1425	16	1502	17	88	5	2,176,639	214,810	625	9,634,952	0.0000	Inc	
90	0.0966	0.0022	0.2829	0.0036	3.7626	0.0857	1558.5	43	1606	19	1585	18	103	22	1,157,825	112,175	4	4,575,889	0.0002	Inc	
91	0.0987	0.0023	0.2744	0.0037	3.7291	0.0859	1599.1	43	1563	19	1578	18	98	35	935,888	93,406	143	3,881,266	0.0004	Inc	
92	0.0993	0.0023	0.2634	0.0036	3.6021	0.0825	1610.9	43	1507	18	1550	18	94	21	273,655	27,538	108	1,172,947	0.0008	Inc	
93	0.0997	0.0026	0.2754	0.0039	3.7788	0.0965	1617.5	48	1568	20	1588	21	97	11	1,194,297	118,707	124	4,905,337	0.0001	Inc	
94	0.0974	0.0021	0.2478	0.0032	3.3247	0.0702	1574.5	40	1427	16	1487	16	91	27	303,011	29,789	168	1,328,016	0.0009	Inc	
95	0.1971	0.0028	0.4371	0.0042	11.8798	0.1518	2802.5	23	2338	19	2595	12	83	548	73,261	14,660	30,042	147,870	0.0374	Exc	c

Notes: a: High $^{204}/^{207}$ ratio; b: Low ^{207}Pb cts.; c: High ^{204}Pb cts.; d: Low ^{238}U cts.

Sample PH-93 was dated at an upper intercept age of 1604 ± 11 Ma with an anchored lower intercept of 0 ± 40 Ma, using a 27- μm spot size and a 12-ppb mixed solution. Sample PH-93 (Figure 5) plots very close to concordia, but displays evidence of slight recent Pb loss like OD10-4. Sample PH-93 was also dated using GJ-1 Zircon as the primary standard, giving an age of 1597.2 ± 6.1 Ma (Figure 5) utilizing 82 of a total of 95 points (Table 4). Although the error is small, the range of discordance is large when compared to the solution analysis, in which spots plot close to or on concordia (Figure 4). The larger spread in PH93 (b) could, however, be due to the larger number of analyses.

Due to its much lower U concentration (average U is 6 ppm), sample CUR-002 was analyzed using a 60- μm spot size and a 1-ppb mixed solution. The sample contains extremely high ^{204}Pb , exemplified by how far the points plot from the lower intercept on the Tera-Wasserburg diagram. The most robust data points, marked in red, have been included in the age regression (Figure 6, Table 5), which produced a lower intercept date of 1707 ± 39 Ma from 40 out of 60 points. When all data are plotted, an age of 1711 ± 120 Ma is produced, excluding two points that gave ^{204}Pb counts which were too high (>700), and one with measured age ratios which were unrealistically old (point 3) and therefore are not included in either date. Despite high levels of ^{204}Pb , the fitted regression line (from ISOPLOT using the algorithm of York, 1969 [18]) produces a low mean square weighted deviation (MSWD) and relatively low error, demonstrating how even samples of very low U and high common Pb can still give geologically meaningful ages.

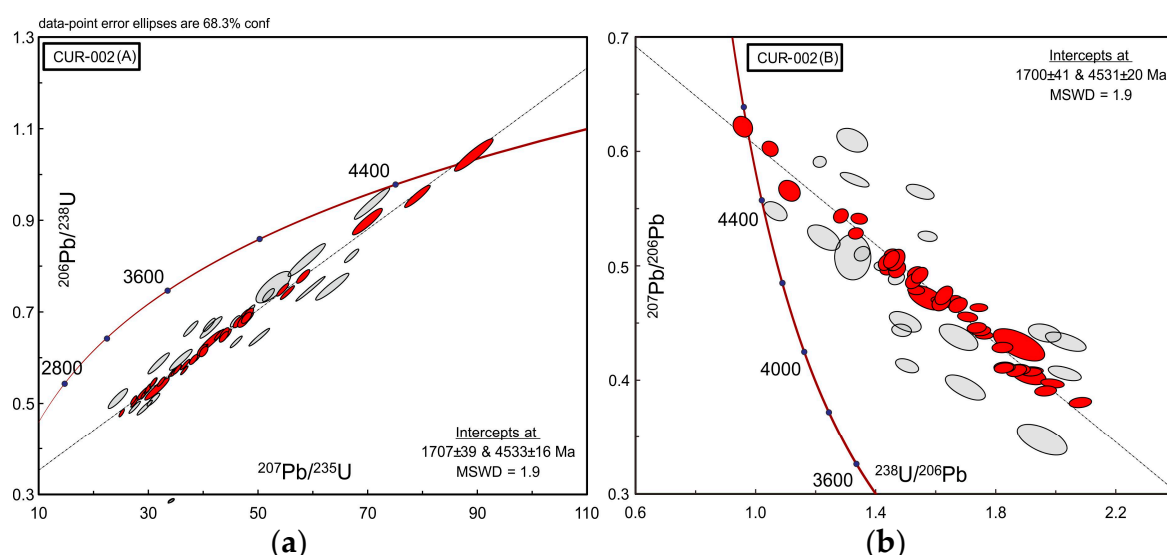


Figure 6. Conventional concordia plot (a) and Tera-Wasserburg diagram (b) for the low-U sample (CUR-002; Carajás, Brazil). The more robust data points marked in red are included in the age regression. Data given in Table 5 as “included” are plotted in red, “excluded” as grey.

Table 5. Geochronological data for zoned hematite (sample CUR-002) using mixed-solution method.

Spot No.	$^{207}\text{Pb}/^{206}\text{Pb}$	1σ	$^{206}\text{Pb}/^{238}\text{U}$	1σ	$^{207}\text{Pb}/^{235}\text{U}$	1σ	$^{207}\text{Pb}/^{206}\text{Pb}$	1σ	$^{206}\text{Pb}/^{238}\text{U}$	1σ	$^{207}\text{Pb}/^{235}\text{U}$	1σ	Concordancy (%)	^{204}Pb	^{206}Pb	^{207}Pb	^{208}Pb	^{238}U	$^{204}\text{Pb}/^{207}\text{Pb}$	Inc/Exc	Notes
1	0.5079	0.0237	0.7545	0.0227	52.8353	2.0992	4264	67	3624	88	4047	45	90	15	695	349	889	1225	0.04298	Exc	
2	0.5755	0.0197	0.7510	0.0179	59.5928	1.7618	4447	49	3611	70	4167	34	87	30	687	391	949	1217	0.07673	Exc	
3	0.7995	0.0107	2.7586	0.0389	304.0886	4.4477	4921	19	8535	74	5809	17	147	265	5445	4307	10,609	2625	0.06153	Exc	a
4	0.4339	0.0162	0.4913	0.0108	29.3881	0.9197	4031	55	2576	49	3467	35	74	30	804	345	1025	2177	0.08696	Exc	
5	0.3478	0.0198	0.5110	0.0143	24.5040	1.1702	3697	84	2661	64	3289	53	81	19	373	128	368	972	0.14844	Exc	
6	0.5249	0.0230	0.8138	0.0237	58.8979	2.2419	4313	63	3838	89	4156	44	92	35	369	191	495	604	0.18325	Exc	
7	0.5480	0.0181	0.9369	0.0226	70.7932	2.1173	4376	48	4262	80	4340	34	98	36	778	421	1083	1105	0.08551	Exc	
8	0.3938	0.0187	0.5880	0.0152	31.9254	1.2866	3886	70	2981	65	3548	45	84	19	416	162	429	941	0.11728	Exc	
9	0.6101	0.0222	0.7556	0.0194	63.5579	1.9968	4532	52	3628	75	4232	36	86	37	562	339	870	989	0.10914	Exc	
10	0.4062	0.0120	0.4921	0.0088	27.5560	0.6905	3932	43	2580	40	3403	28	76	8	1217	488	1594	3289	0.01639	Exc	
11	0.5650	0.0162	0.6452	0.0128	50.2601	1.2436	4420	41	3209	53	3997	28	80	38	1003	560	1500	2068	0.06786	Exc	
12	0.4724	0.0195	0.6368	0.0160	41.4764	1.4602	4157	60	3176	66	3807	40	83	13	455	212	545	951	0.06132	Inc	
13	0.4312	0.0239	0.5323	0.0160	31.6463	1.4703	4022	80	2751	70	3539	52	78	8	342	146	367	856	0.05479	Inc	
14	0.4377	0.0196	0.5959	0.0151	35.9663	1.3620	4044	65	3013	64	3666	43	82	13	398	172	430	888	0.07558	Exc	
15	0.5415	0.0091	0.7428	0.0100	55.4611	0.8533	4358	24	3581	39	4096	18	87	141	4477	2394	5560	8013	0.05890	Inc	
16	0.5260	0.0092	0.6350	0.0085	46.0560	0.7213	4316	25	3169	35	3911	18	81	82	2763	1435	3412	5785	0.05714	Exc	
17	0.6219	0.0175	1.0434	0.0234	89.4817	2.3285	4560	40	4607	79	4574	30	101	31	816	507	1251	1028	0.06114	Inc	
18	0.6026	0.0128	0.9530	0.0161	79.1910	1.5412	4514	30	4315	57	4452	22	97	39	1436	865	2136	1982	0.04509	Inc	
19	0.5659	0.0162	0.8979	0.0191	70.0616	1.8009	4423	41	4131	69	4329	30	95	15	953	539	1332	1397	0.02783	Inc	
20	0.4046	0.0134	0.5231	0.0103	29.1756	0.8171	3926	49	2712	46	3459	31	78	22	1246	504	1187	3135	0.04365	Inc	
21	0.4512	0.0169	0.6666	0.0156	41.4718	1.3298	4089	54	3293	64	3807	36	86	36	706	318	837	1393	0.11321	Exc	
22	0.4556	0.0079	0.5857	0.0076	36.7934	0.5699	4104	26	2972	33	3688	18	81	85	3205	1458	3389	7199	0.05830	Inc	
23	0.4090	0.0059	0.5192	0.0060	29.2778	0.3877	3942	22	2696	27	3463	15	78	113	5986	2444	5153	15,168	0.04624	Inc	
24	0.4637	0.0061	0.5731	0.0064	36.6418	0.4497	4130	19	2920	28	3684	14	79	228	8706	4031	9108	19,990	0.05656	Inc	
25	0.4704	0.0062	0.6199	0.0070	40.2129	0.4940	4151	19	3110	29	3776	14	82	207	8683	4077	9156	18,431	0.05077	Inc	
26	0.4395	0.0057	0.5672	0.0063	34.3697	0.4176	4050	19	2896	27	3621	14	80	185	9174	4023	8902	21,285	0.04599	Inc	
27	0.3975	0.0073	0.5024	0.0065	27.5376	0.4435	3900	27	2624	29	3403	18	77	90	4110	1630	3469	10,768	0.05521	Inc	
28	0.4998	0.0075	0.7029	0.0086	48.4418	0.6644	4241	22	3431	34	3961	16	87	110	4804	2395	5666	8995	0.04593	Exc	
29	0.4129	0.0109	0.6638	0.0112	37.7835	0.8694	3957	39	3282	46	3714	26	88	29	1052	433	1124	2086	0.06697	Exc	
30	0.4790	0.0071	0.6511	0.0079	42.9972	0.5849	4178	22	3232	32	3842	15	84	140	4823	2303	5181	9752	0.06079	Inc	
31	0.5911	0.0081	0.8230	0.0098	67.0843	0.8588	4486	20	3871	37	4286	15	90	244	6976	4110	9492	11,159	0.05937	Exc	
32	0.4414	0.0129	0.5088	0.0093	30.9697	0.7696	4056	43	2652	42	3518	28	75	36	1206	530	1572	3121	0.06792	Exc	
33	0.4970	0.0064	0.6938	0.0082	47.5389	0.6026	4232	19	3397	33	3942	14	86	257	9016	4565	10,418	18,473	0.05630	Inc	
34	0.5287	0.0072	0.7490	0.0092	54.5962	0.7268	4323	20	3604	36	4080	15	88	174	7320	3942	9031	13,891	0.04414	Inc	
35	0.5094	0.0085	0.6856	0.0091	48.1500	0.7354	4269	24	3366	37	3955	17	85	36	3437	1783	4112	7126	0.02019	Inc	
36	0.4075	0.0052	0.5208	0.0061	29.2629	0.3683	3937	19	2703	27	3462	14	78	259	11,938	4954	10,495	32,573	0.05228	Inc	
37	0.4097	0.0065	0.5319	0.0068	30.0497	0.4415	3945	23	2750	30	3488	17	79	115	4992	2082	4365	13,336	0.05524	Inc	
38	0.4434	0.0059	0.5706	0.0069	34.8889	0.4528	4063	20	2910	30	3636	15	80	248	10,188	4598	10,140	25,363	0.05394	Inc	
39	0.4438	0.0086	0.6720	0.0098	41.1226	0.7212	4065	28	3313	40	3798	20	87	72	3388	1530	3761	7163	0.04706	Exc	
40	0.3807	0.0051	0.4800	0.0057	25.1978	0.3247	3835	20	2527	26	3316	14	76	208	10,362	4014	8264	30,661	0.05182	Inc	
41	0.5439	0.0077	0.7781	0.0099	58.3534	0.7965	4365	21	3710	38	4146	16	89	211	6461	3575	8414	11,794	0.05902	Inc	
42	0.4461	0.0061	0.5755	0.0070	35.3955	0.4646	4072	20	2930	30	3650	15	80	215	9036	4100	9398	22,298	0.05244	Inc	
43	0.3909	0.0055	0.5083	0.0062	27.3917	0.3676	3874	21	2649	27	3398	15	78	224	9642	3832	8136	26,937	0.05846	Inc	
44	0.4289	0.0064	0.5484	0.0069	32.4251	0.4558	4014	22	2818	30	3563	16	79	161	6409	2795	6425	16,595	0.05760	Inc	
45	0.4938	0.0064	0.6516	0.0078	44.3641	0.5614	4223	19	3235	32	3873	14	84	325	11,453	5750	13,157	24,955	0.05652	Inc	

Table 5. Cont.

Spot No.	$^{207}\text{Pb}/^{206}\text{Pb}$	1σ	$^{206}\text{Pb}/^{238}\text{U}$	1σ	$^{207}\text{Pb}/^{235}\text{U}$	1σ	$^{207}\text{Pb}/^{206}\text{Pb}$	1σ	$^{206}\text{Pb}/^{238}\text{U}$	1σ	$^{207}\text{Pb}/^{235}\text{U}$	1σ	Concordancy (%)	^{204}Pb	^{206}Pb	^{207}Pb	^{208}Pb	^{238}U	$^{204}\text{Pb}/^{207}\text{Pb}$	Inc/Exc	Notes
46	0.4894	0.0065	0.6799	0.0082	45.8711	0.5930	4210	19	3344	33	3907	15	86	279	10,540	5243	11,951	22,008	0.05321	Exc	
47	0.8669	0.0088	0.2860	0.0031	34.1905	0.3687	5036	14	1622	16	3616	12	45	777	13,952	12,306	30,244	69,651	0.06314	Exc	b
48	0.4972	0.0072	0.6791	0.0086	46.5568	0.6617	4233	21	3341	35	3921	16	85	313	9793	4954	11,138	20,592	0.06318	Inc	
49	0.5108	0.0072	0.7374	0.0093	51.9359	0.7105	4273	21	3561	37	4030	16	88	197	7059	3669	8418	13,670	0.05369	Exc	
50	0.5035	0.0068	0.6961	0.0086	48.3154	0.6385	4251	20	3406	34	3958	15	86	233	8236	4219	9461	16,898	0.05523	Inc	
51	0.4086	0.0052	0.5346	0.0063	30.1152	0.3762	3941	19	2761	27	3491	14	79	235	12,837	5336	11,538	34,294	0.04404	Inc	
52	0.4116	0.0064	0.5463	0.0070	31.0008	0.4509	3952	23	2810	30	3519	16	80	131	5235	2192	4653	13,684	0.05976	Inc	
53	0.4689	0.0061	0.6022	0.0072	38.9287	0.4980	4146	19	3039	30	3744	14	81	221	9413	4490	10,079	22,322	0.04922	Inc	
54	0.5037	0.0070	0.6836	0.0085	47.4700	0.6426	4252	20	3358	35	3941	15	85	185	6693	3430	7921	13,983	0.05394	Inc	
55	0.4660	0.0062	0.5967	0.0072	38.3383	0.4977	4137	20	3017	31	3729	15	81	228	9452	4481	10,003	22,618	0.05088	Inc	
56	0.4682	0.0068	0.6175	0.0077	39.8614	0.5506	4144	21	3100	32	3767	16	82	169	6028	2871	6551	13,941	0.05886	Inc	
57	0.5054	0.0081	0.6809	0.0092	47.4539	0.7169	4257	23	3348	37	3940	17	85	128	5101	2623	6203	10,697	0.04880	Inc	
58	0.4745	0.0062	0.6141	0.0074	40.1715	0.5132	4164	19	3086	31	3775	14	82	271	10,198	4922	11,044	23,715	0.05506	Inc	
59	0.4109	0.0053	0.5469	0.0064	30.9847	0.3917	3950	19	2812	28	3519	14	80	207	11,033	4612	9957	28,810	0.04488	Inc	
60	0.4873	0.0063	0.6545	0.0078	43.9712	0.5584	4203	19	3246	32	3865	14	84	276	9859	4887	11,148	21,511	0.05648	Inc	
61	0.5060	0.0064	0.6879	0.0082	47.9915	0.6050	4259	19	3375	33	3952	14	85	312	11,239	5786	13,189	23,331	0.05392	Inc	
62	0.4921	0.0061	0.6461	0.0076	43.8357	0.5412	4218	18	3213	31	3862	14	83	289	12,589	6302	14,254	27,823	0.04586	Inc	
63	0.8656	0.0088	0.2867	0.0031	34.2216	0.3698	5034	14	1625	16	3616	12	45	759	13,760	12,118	29,798	68,525	0.06263	Exc	b

Notes: a: Age ratios too high; b: High ^{204}Pb cts.

5. Discussion

5.1. Advantages of the Mixed-Solution Method and Comparison of Data with GJ-1 Zircon

Dating of the same hematite sample from the Olympic Dam high-grade ore (OD-10), using the GJ-1 Zircon calibration and the U–Pb solution method, produced ages that are statistically identical (1577 ± 5 Ma and 1595 ± 18 Ma). The larger error using the mixed-solution method is most likely attributable to the reduced size of the dataset (all 15 data points obtained are displayed in Figure 5, whereas 116 spots were included, and 97 rejected by Ciobanu et al. (2013)) [3]. Statistical overlaps between $^{207}\text{Pb}/^{206}\text{Pb}$ weighted average ages (using GJ-1 Zircon) and U/Pb upper intercept ages (using the U–Pb mixed solution method) demonstrate that, although fractionation associated with a non-matrix matched standard does occur when using zircon as the primary standard, it does not impact the $^{207}\text{Pb}/^{206}\text{Pb}$ or intercept age. GJ-1 Zircon can thus be considered reliable for dating hematite by LA-ICP-MS. The data acquired in this study via the mixed solution method minimises these matrix effects and is considered more reliable since all analyzed points could be included.

The dates obtained for sample PH93 also overlap statistically (1597.2 ± 6.1 Ma vs. 1604 ± 11 Ma when using GJ-1 Zircon and mixed solution standards, respectively). The larger error for the mixed-solution method can again be attributed to the smaller dataset. Of importance here is the fact that, unlike the U–Pb mixed-solution date, the $^{207}\text{Pb}/^{206}\text{Pb}$ GJ-1 Zircon age features data points that plot very far along the discordia (Figure 5). This clearly highlights the reduction in matrix effects by using the mixed-solution method. Both examples of high-U hematite show that the mixed-solution method used here can give higher quality data from the majority of analyzed points.

An important result of this study is that when using either the GJ-1 Zircon calibration or the solution method for the same samples (high-U, Olympic Cu-Au Province hematite), the majority of data plot either below or above the concordia. In both cases, however, data points that intercept the concordia are also obtained. Data points above concordia can be attributed to an increase in the $^{206}\text{Pb}/^{238}\text{U}$ ratio due to downhole fractionation effects (Figure 7), a phenomenon also observed in zircon spot analysis by Paton et al. (2010) [19]. In this study, such an effect cannot be corrected for via modeling of the downhole fractionation whilst ablating the standard, as the U and Pb analyzed is not contained within the pure $\alpha\text{-Fe}_2\text{O}_3$ matrix ablated, but rather introduced as a solution, and thus the U/Pb ratio remains unaffected by laser induced fractionation during ablation (Figure 7). The results here also place further constraints on the GJ-1 Zircon calibration method, where data points plotting below concordia can be mostly attributed to effects of matrix mismatch (different levels of U fractionation between zircon and hematite). In both cases, however, there is uncertainty about the relative loss or addition of U (open system behavior), which cannot be solved by either method.

By including the low-U concentration Brazilian sample (6 ppm) in our study (CUR-002), we have shown that the solution method has advantages over the GJ-1 Zircon calibration method, and has wide application to analysis of samples containing low concentrations of U (tens of ppm or less). Following this, it is reasonable to assume that samples of comparable U concentration can be dated by this method, opening up considerable scope for very low U age determinations elsewhere.

Although downhole fractionation was likely occurring during analysis of the CUR-002 sample, the large spread through the discordia (Figure 6) is predominantly due to the high amount of common Pb contained within these grains, as attested to by the high ^{204}Pb measured during analysis. Of importance here, is that we have shown how samples of such low U concentration, can only be considered suitable for dating through the U–Pb solution method, which can be tailored to accommodate the significantly lower U concentrations. This is because GJ-1 Zircon and other zircon standards have much higher U concentrations, relative to this sample, or others with similarly low-U concentrations, creating potential matrix effects when employed as the primary standard.

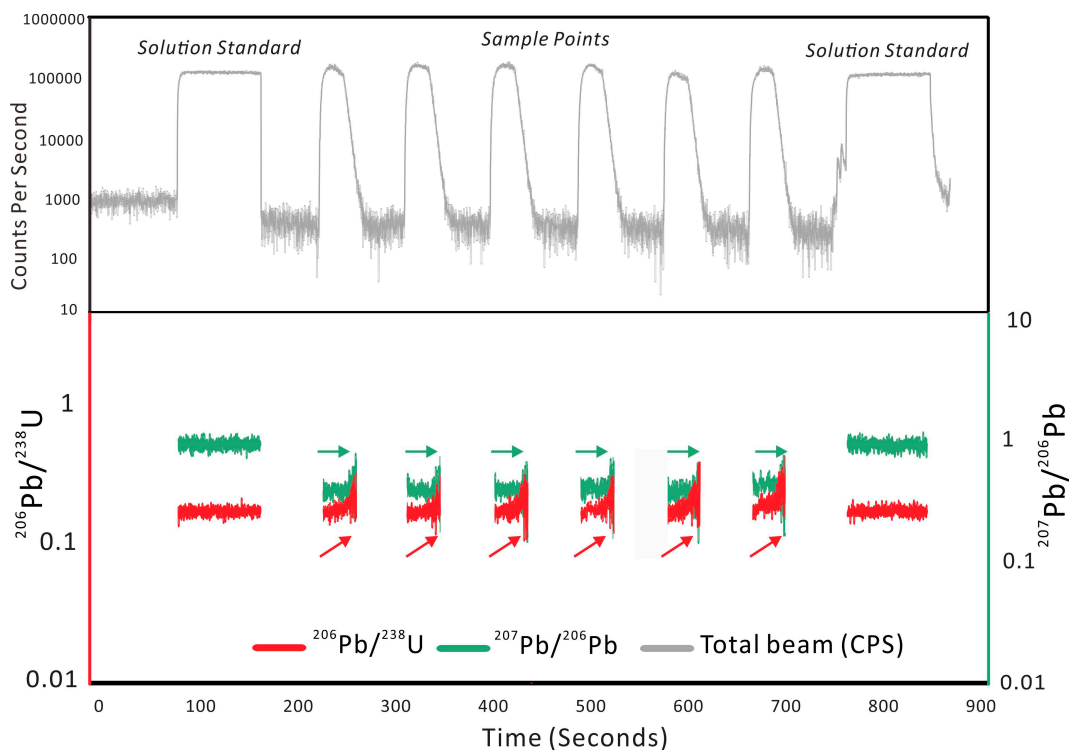


Figure 7. Time-resolved spectra data produced using IOLITE from data obtained from hematite in Olympic Cu-Au Province samples. Note no downhole fractionation within the solution standard, but significant fractionation of the $^{206}\text{Pb}/^{238}\text{U}$ ratio (red), which increases with time during the duration of the spot analysis. The $^{207}\text{Pb}/^{206}\text{Pb}$ ratio (green) remains relatively constant throughout analysis, showing the robustness of the $^{207}\text{Pb}/^{206}\text{Pb}$ ages. This represents a minor disadvantage of the method but may be overcome in the future through linear rastering rather than spot analysis, if the homogeneity of the analyzed grain allows this.

5.2. Geologic Meaning of the Hematite Ages

The geological significance of the Olympic Dam hematite ages has been amply discussed in [3] and references therein, and supports formation of IOCG systems in South Australia coeval with LIP magmatism (Hiltaba Intrusive Suite and Gawler Range Volcanics) at ~1.6 Ga.

In contrast to relatively abundant data for the Olympic Dam District, supportive geochronological data for other deposits in the Olympic Cu-Au Province deposit remains sparse. The 1597.2 ± 6.1 Ma hematite date obtained using GJ-1 Zircon as the primary standard does not overlap with a published U/Pb zircon crystallization ages of 1586 ± 3 Ma for an associated granite from the central Mount Woods Inlier [20], but does statistically overlap with the of 1587 ± 4 Ma date obtained for a cumulate gabbronorite [20]. Although the mixed-solution U-Pb hematite date (1604 ± 11 Ma) is statistically different to published ages, it is nonetheless very close. Minor differences in absolute age could be attributed to a non-direct relationship between the hematite associated with mineralization and LIP magmatism in the area. Most importantly, the present data for PH93 is further argument for the importance of the ~1.6 Ga IOCG event throughout the Olympic Cu-Au Province.

The date obtained for the Brazilian sample (1707 ± 39 Ma) is within the range of geological events associated with the Carajás mineral province (1.80 Ga U/Pb zircon ages from A-type magmatism at the Carajás Granite [16], and 1.61 Ga U/Pb zircon ages from rift-related granitic magmatism [17]). The hematite dated here could represent a vein-related mineralizing event, but needs to be corroborated by data on samples with less common Pb or by using dating methods, such as ID-TIMS, for more accurate age determination. Regardless, the date obtained in this study is similar to the other ages considered for the protracted tectono-magmatic history of the Carajás mineral province [21].

6. Implications and Outlook

This study has successfully established a new matrix-matched dating method for hematite using a U–Pb mixed solution/pure hematite standard. Through the decreased matrix effects, homogeneity of the solution and tailoring of U concentration differences between the sample and standard, a set of reliable dates have been obtained. The Fe-oxide hematite can now be dated using a U–Pb mixed solution/pure hematite standard method that provides high signal stability and has broad application to low-U samples. The samples will be further evaluated by ID-TIMS, to show whether the apparent discordance is due to the problems associated with the analytical methods used so far (e.g., Matrix-effects and downhole fractionation) or open system behavior. Although the zircon standardized data does show increased U/Pb fractionation, most likely due to matrix effects, the upper intercept ages are still statistically the same as that of the solution method, making the GJ-1 Zircon standard reliable for obtaining upper intercept and ^{207}Pb - ^{206}Pb weighted average ages. Using the mixed solution method, we have also validated the original age obtained for OD-10 [3]. We have demonstrated that although the use of GJ-1 Zircon as the primary standard does create more “apparent” fractionation with greater spreading of analytical points down the discordia, the upper intercept and weighted average ^{207}Pb - ^{206}Pb dates obtained are still geologically meaningful. To eliminate downhole fractionation associated with the solution method, we will analyze samples using a line raster. This was not carried out in the analytical session described in this paper because of the lack of current samples exhibiting the same high U zonation patterns with large enough grains to carry out this type of analysis.

Further research includes finding suitable material for a solid hematite standard so that other more-precise microbeam methods, including SHRIMP, can be routinely used for dating. The mixed solution standard method presented here will also be applied to U-bearing magnetite following similar procedures. The petrographic and genetic link between Fe-oxides and hydrothermal mineralization is one that can be directly correlated when compared to other mineral geochronometers, such as monazite and zircon, making this study an important step towards establishing U–Pb iron-oxide geochronology as a valuable tool that can be routinely used to constrain the genesis of mineral deposits.

Supplementary Materials: The following are available online at www.mdpi.com/2075-163X/6/3/85/s1, Supplementary Text File S1: Additional analytical procedures for calculating and certifying the Pb/U ratios; Table S1: Pb isotope ratios of Pb standard solution; Table S2: U and Pb concentrations in standard solutions; Table S3: Correlation coefficient of the regression line.

Acknowledgments: This work is a contribution to the “FOX” project (Trace elements in iron oxides: deportment, distribution and application in ore genesis, geochronology, exploration and mineral processing), supported by BHP Billiton Olympic Dam and the S.A. Mining and Petroleum Services Centre of Excellence. Alexandre R. Cabral gratefully acknowledges VALE S.A. for financing his research position at the Technische Universität Clausthal and for logistically supporting his fieldwork in Carajás. We also gratefully acknowledge Yang Tao and Yan Xiong for their assistance with lead isotope analysis at the State Key Laboratory for Mineral Deposits Research, Department of Earth Sciences, Nanjing University, China.

Author Contributions: Zhiyong Zhu conceived and designed the experiments; Liam Courtney-Davies, Zhiyong Zhu and Cristiana L. Ciobanu performed the experiments under the guidance of Benjamin P. Wade. Liam Courtney-Davies, Zhiyong Zhu and Benjamin P. Wade processed the data; Kathy Ehrig and Alexandre R. Cabral contributed samples and information; Liam Courtney-Davies, Zhiyong Zhu, Cristiana L. Ciobanu and Nigel J. Cook wrote the paper, assisted by Benjamin P. Wade, Allen Kennedy and Kathy Ehrig. The work is part of the PhD project of Liam Courtney-Davies. We would also like to thank two anonymous reviewers for their detailed thoughts and important amendments, which helped us to clarify our interpretations, along with Matthew Horstwood with whom conversations further aided this study.

Conflicts of Interest: The authors declare no conflict of interest. The project sponsors approve publication of the manuscript.

References

1. Jackson, S.E.; Pearson, N.J.; Griffin, W.L.; Belousova, E.A. The application of laser ablation inductively coupled plasma-mass spectrometry to in-situ U–Pb zircon geochronology. *Chem. Geol.* **2004**, *211*, 47–69. [[CrossRef](#)]

2. McFarlane, C.R.M.; Luo, Y. U-Pb Geochronology Using 193 nm Excimer LA-ICP-MS Optimized for In-Situ Accessory Mineral Dating in Thin Sections. *Geosci. Can. Anal. Tech. Ser.* **2012**, *39*, 158–172.
3. Ciobanu, C.L.; Wade, B.P.; Cook, N.J.; Schmidt Mumm, A.; Giles, D. Uranium-bearing hematite from the Olympic Dam Cu-U-Au deposit, South Australia; a geochemical tracer and reconnaissance Pb-Pb geochronometer. *Precambr. Res.* **2013**, *238*, 129–147. [[CrossRef](#)]
4. Johnson, J.P.; Cross, K.C. U-Pb geochronological constraints on the genesis of the Olympic Dam Cu-U-Au-Ag deposit, South Australia. *Econ. Geol.* **1995**, *90*, 1046–1063. [[CrossRef](#)]
5. Günther, D.; Heinrich, C.A. Enhanced sensitivity in laser ablation-ICP mass spectrometry using helium-argon mixtures as aerosol carrier. *J. Anal. At. Spectrom.* **1999**, *14*, 1363–1368. [[CrossRef](#)]
6. Becker, J.S. State-of-the-art and progress in precise and accurate isotope ratio measurements by ICP-MS and LA-ICP-MS. *Plenary Lecture. Anal. At. Spectrom.* **2002**, *17*, 1172–1185. [[CrossRef](#)]
7. Günther, D. Laser Ablation-Inductively Coupled Plasma Mass Spectrometry Trends. *Anal. Bioanal. Chem.* **2002**, *372*, 31–32. [[CrossRef](#)]
8. Horn, I.; Rudnick, R.L.; McDonough, W.F. Precise elemental and isotope ratio determination by simultaneous solution nebulization and laser ablation-ICP-MS: application to U-Pb geochronology. *Chem. Geol.* **2000**, *164*, 281–301. [[CrossRef](#)]
9. Košler, J.; Fonneland, H.; Sylvester, P.; Tubrett, M.; Pedersen, R.-B. U-Pb dating of detrital zircons for sediment provenance studies—A comparison of laser ablation ICPMS and SIMS techniques. *Chem. Geol.* **2002**, *182*, 605–618. [[CrossRef](#)]
10. Simonetti, A.; Heaman, L.M.; Hartlaub, R.P.; Creaser, R.A.; MacHattie, T.G.; Böhm, C. U-Pb zircon dating by laser ablation MC-ICP-MS using a new multiple ion counting Faraday collector array. *J. Anal. At. Spectrom.* **2005**, *20*, 677–686. [[CrossRef](#)]
11. Leach, J.J.; Allen, L.A.; Aeschliman, D.B.; Houk, R.S. Calibration of Laser Ablation ICP-MS Using Standard Additions with Dried Solution Aerosols. *Anal. Chem.* **1999**, *71*, 440–445. [[CrossRef](#)]
12. Pickhardt, C.; Becker, J.S.; Dietze, H.J. A new strategy of solution calibration in laser ablation inductively coupled plasma mass spectrometry for multi element trace analysis of geological samples. *J. Anal. Chem.* **2000**, *368*, 173–181. [[CrossRef](#)]
13. Van Achterbergh, E.; Ryan, C.; Jackson, S.; Griffin, W. Appendix 3 Data reduction software for LA-ICP-MS. In *Laser-Ablation-ICPMS in the Earth Sciences*; Sylvester, P., Ed.; Mineralogical Association of Canada: Quebec City, QC, Canada, 2001; Volume 29, pp. 239–243.
14. Ludwig, K.R. *A User's Manual for Isoplot 3.75: A Geochronological Toolkit for Microsoft Excel*; Berkeley Geochronology Centre Special Publication No.5; Berkeley Geochronology Centre: Berkeley, CA, USA, 2012.
15. White, W.M.; Albarède, F.; Télouk, P. High-precision analysis of Pb isotope ratios by multi-collector ICP-MS. *Chem. Geol.* **2000**, *167*, 257–270. [[CrossRef](#)]
16. Machado, N.; Lindenmayer, Z.; Krogh, T.E.; Lindenmayer, D. U-Pb geochronology of Archean magmatism and basement reactivation in the Carajás area, Amazon Shield, Brazil. *Precambr. Res.* **1991**, *49*, 329–354. [[CrossRef](#)]
17. Pimentel, M.M.; Heaman, L.; Fuck, R.A.; Marini, O.J. U-Pb zircon geochronology of Precambrian tin-bearing continental-type acid magmatism in central Brazil. *Precambr. Res.* **1991**, *52*, 321–335. [[CrossRef](#)]
18. York, D. Least-squares fitting of a straight line with correlated errors. *Earth Plan. Sci. Lett.* **1969**, *5*, 320–324. [[CrossRef](#)]
19. Paton, C.; Woodhead, J.D.; Hellstrom, J.C.; Hergt, J.J.; Greig, A.; Maas, R. Improved laser ablation U-Pb zircon geochronology through robust downhole fractionation correction. *Geochem. Geophys. Geosyst.* **2010**, *11*, 1–36. [[CrossRef](#)]
20. Jagodzinski, E.A. Compilation of SHRIMP U-Pb geochronological data, Olympic Domain, Gawler Craton, South Australia, 2001–2003. *Geosci. Aust. Rec.* **2005**, *20*, 211.
21. Pinheiro, R.V.L.; Holdsworth, R.E. Reactivation of Archaean strike-slip fault systems, Amazon region, Brazil. *J. Geol. Soc.* **1997**, *154*, 99–103. [[CrossRef](#)]

